Microbial Cell Factories

RESEARCH Open Access

Promoter engineering with programmable upstream activating sequences in *Aspergillus Niger* cell factory

Xiaomei Zheng[1,2,3,4], Yuting Guo[1,2,4], Meiling Chen[1,2,5], Yudan Lu[1,2,4], Yimou Du[1,2,4], Yu Lei[1,4], Ping Zheng[1,2,3,4*] and Jibin Sun[1,2,3,4*]

Abstract

Background *Aspergillus niger* is an important industrial filamentous fungus used to produce organic acids and enzymes. A wide dynamic range of promoters, particularly strong promoters, are required for fine-tuning the regulation of gene expression to balance metabolic flux and achieve the high yields of desired products. However, the limited understanding of promoter architectures and activities restricts the efficient transcription regulation of targets in strain engineering in *A. niger*.

Results In this study, we identified two functional upstream activation sequences (UAS) located upstream of the core promoters of highly expressed genes in *A. niger*. We constructed and characterized a synthetic promoter library by fusing the efficient UAS elements upstream of the strong constitute P*gpdA* promoter in *A. niger*. It demonstrated that the strength of synthetic promoters was fine-tuned with a wide range by tandem assembly of the UAS elements. Notably, the most potent promoter exhibited 5.4-fold higher activity than the strongest P*gpdA* promoter reported previously, significantly extending the range of strong promoters. Using citric acid production as a case study, we employed the synthetic promoter library to enhance citric acid efflux by regulating the *cexA* expression in *A. niger*. It showed a 1.6-2.3-fold increase in citric acid production compared to the parent strain, achieving a maximum titer of 145.3 g/L.

Conclusions This study proved that the synthetic promoter library was a powerful toolkit for precise tuning of transcription in *A. niger*. It also underscores the potential of promoter engineering for gene regulation in strain improvement of fungal cell factories.

Keywords *Aspergillus Niger*, Synthetic promoter, Upstream activation sequence, Fluorescence protein, Citric acid production

*Correspondence:
Ping Zheng
zheng_p@tib.cas.cn
Jibin Sun
sun_jb@tib.cas.cn
[1]Tianjin Institute of Industrial Biotechnology, Chinese Academy of Sciences, Tianjin 300308, China
[2]National Center of Technology Innovation for Synthetic Biology, Tianjin 300308, China
[3]University of Chinese Academy of Sciences, Beijing 100049, China
[4]College of Biotechnology, Tianjin University of Science & Technology, Tianjin 300457, China
[5]School of Biotechnology, East China University of Science and Technology, Shanghai 200237, China

Background

Aspergillus niger is an essential industrial filamentous fungus and has been extensively developed as a fungal cell factory for the biomanufacturing of organic acids and enzymes, including citric acid, gluconic acid, amylase, and glucoamylase [1–3]. For instance, *A. niger* serves as the primary workhorse for the citric acid industry, which boasts a global market of nearly 2.0 million tons [2]. Currently, the rapid developments of the Clustered Regularly Interspaced Short Palindromic Repeats (CRISPR)/CRISPR associated (Cas) system-mediated genome editing techniques [4–6] have efficiently removed bottlenecks in genetic manipulation, accelerating the iterative improvement of this fungal cell factory.

In addition to genetic manipulation toolboxes, precise regulation of gene expression is vital to optimize complex metabolic pathways and maximize the yields of desired products [7]. Promoters, as fundamental regulatory elements of transcription, are exploited to fine-tune gene expression in fungi [8–11]. Similar to the Q-system from *Neurospora crassa* widely used across species [12–15], several heterologous bacterial promoter systems, such as the doxycycline-inducible Tet-ON/Tet-OFF system [16, 17] and the universal SES system [18], have been successfully utilized in fungi. Given the requirement for strong and stable gene expression, low production cost and simple fermentation control in industrial biomanufacturing, several native promoters have been identified and applied for metabolic engineering in *A. niger*, including the inducible glucoamylase promoter (P*glaA*) [19, 20], the multiprotein bridging factor promoter P*mbfA* [8], and the glyceraldehyde-3-phosphate dehydrogenase promoter (P*gpdA*) [11]. Among these promoters, the strong constitutive P*gpdA* promoter has been widely used for optimizing metabolic pathways in *A. niger* [11, 21]. The overexpression of citrate exporter gene *cexA* driven by the native P*gpdA* promoter achieved a 2.48-fold increase in citric acid production [11]. Similarly, the overexpression of NAD kinases Utr1p using P*gpdA* optimized the NADPH availability, resulting in a significant improvement of malic acid titer of 110.7 g/L compared to the parent strain (85.0 g/L) [21].

Regarding promoter architectures, fungal promoters are notably longer than prokaryotic promoters, typically exceeding 500 bp, and more complicated but contain conserved elements that vary between species [22]. Many yeast promoters are well-defined and often sought after, typically consisting of core promoter elements and upstream activation sequences (UASs) [7]. UAS elements upstream of the core promoters serve as binding sites for specific transcriptional activators, facilitating gene expression activation [22, 23]. Many UAS elements have been identified in yeast, including UASTEF [24], UASCLB [25], UASCIT [26], UASTDH3 [27] in *Saccharomyces cerevisiae*, UAS1B [28] in *Yarrowia lipolytica*, and UAS1^{Y13}, UAS2^{Y13}, UAS1^{Y14}, UAS2^{Y14} in *Ogataea polymorpha* [29]. These UAS elements have been successfully exploited to construct synthetic hybrid promoters and improve promoter strength in yeast [23, 27, 29–31]. For instance, the addition of the native UAS1 and UAS2 in the growth phase-dependent promoters Pro-Y13 and Pro-Y14 resulted in 2.0-fold increases in promoter activity in *O. polymorpha* [29]. However, only a few potential promoter-enhanced sequences have been evaluated in filamentous fungi, including 83-bp CCAAT-containing sequence of the P*glaA* promoter in *A. niger* [32], GpdA-box of the P*gpdA* promoter in *Aspergillus nidulans* [33] and a Region III sequence in the P*agdA* promoter of *Aspergillus oryzae* [34]. For instance, the P*agdA142* promoter containing 12 tandem repeats of Region III showed higher activity with an increase of 5.0-fold in comparison with the intrinsic promoter (P*agdA*) in *A. oryzae*, suggesting Region III may function as a UAS element [34]. There is a knowledge gap in the comprehensive understanding of the native promoter architectures, restricting the design and development of synthetic promoters in filamentous fungi.

To address these issues, we identified three UAS elements from the promoter sequences of highly expressed genes encoding amylolytic enzymes. We evaluated their impact on promoter activity by fusing these UAS elements upstream of the native strong constitute promoter P*gpdA*. The promoter evaluation workflow, featuring an intuitive fluorescent-auxotrophic double selection [11], combined with the CRISPR/Cas9 system and flow cytometry, was used to assess the strength of synthetic promoters accurately. We constructed a library through the tandem assembly of functional UAS elements to generate synthetic promoters with a broad activity range, resulting in a series of strong synthetic promoters. We further assessed the versatility of the identified UAS elements by fusing them with different core promoter elements of the promoters P*citA* and P*pkiA*. Finally, we applied this synthetic promoter library to regulate citric acid efflux, significantly improving citric acid production compared to the previously reported strong promoter P*gpdA*. This novel synthetic promoter library based on the identified UAS elements not only provided particularly efficient gene regulatory elements for metabolic engineering in *A. niger* but also provided a reference for mining functional UAS elements and establishing synthetic promoter libraries in other fungal cell factories.

Methods

Strains and cultivation conditions

The strains used in this study are listed in Table S1. *Escherichia coli* DH5α (Transgene, Beijing, China) was used for plasmid construction and cultured at 37 °C

in Luria-Bertani broth containing ampicillin (100 μg/mL). The citric acid-producing strain *A. niger* D353.8 (*kusA::hph*, *pyrG::hph*, *hyg*^{R}) was stored in the lab [35]. *A. niger* strains were cultivated on complete medium (CM) or defined minimal medium (MM), as reported previously [36]. 1.5% agar was supplemented for plates. Ten mM uracil was supplemented in the media for the *pyrG* mutants when necessary.

DNA construction

The plasmids, protospacers, primers, and DNA sequences of the UAS elements used in this study were shown in Table S2-Table S5, respectively. Three predicted UAS elements, UASa, UASb, and UASc, were individually fused to the core element of the P*gpdA* promoter from *A. niger*. UASa, UASb, and UASc represented UASamyA, UASagdA and UASglaA, respectively (Table S5). The promoter reporting plasmid pYT1 was constructed by the reverse PCR with the primers pYT-rev-F and pYT-rev-R, using pYDD2 as a template. The primers were designed to contain the 70-bp or 80-bp UAS elements, such as UASa-F1 and UASa-R1 (Table S4), which were used for PCR amplification with the template of pYT1. The synthetic promoters reporting plasmids pYT2-pYT4 were generated with the UASa, UASb, and UASc elements, respectively (Table S2).

To increase the copy number of UAS elements, the primers with overlapping DNA sequences were designed and used for PCR (Figure S1). Taking UASa as an example, the first round of PCR was conducted using the primers of UASa-F2 and UASa-R2 (Table S4) for self-annealing and amplification to generate a series of tandem UASa elements (Table S5). The first round of PCR product was used as the template for the second round of PCR, with the primers of UASa-F3 and UASa-R3 (Table S4). These DNA fragments with different copies of UAS elements (Table S5) were purified and cloned into the backbone of the reporting plasmids pYT1 and pYT2, using the ClonExpress™ one-step cloning kit (Vazyme, C113), generating pYT5-pYT20, respectively (Table S2). To investigate the compatibility between the UAS elements and the core promoter elements, the core elements of the P*citA* and P*pkiA* promoters were amplified with the primers PcitA-F/PcitA-R and PpkiA-F/PpkiA-R to replace the core element of the P*gpdA* promoter in the plasmids pYT1, pYT3, pYT13, and pYT15, respectively. For the P*citA* promoter, the pYT21-pYT24 were constructed without and with One, two, and four copies of the UASb element, respectively (Table S2). For the P*pkiA* promoters, the pYT25-pYT28 were constructed with the same design (Table S2).

Similarly, the DNA fragments with two hybrid UAS elements (Table S5) were amplified using the corresponding primers, such as UASab-F and UASab-R, which were also used as the template of the second round of PCR, to generate hybrid UAS elements. These DNA fragments with hybrid UAS elements were also inserted into the background of the pYT2 and pYT3 plasmids, generating pYT29-pYT35, respectively (Table S2). These plasmids were used as templates for generating donor DNA containing the *mCherry-pyrG* expression cassettes driven by different synthetic promoters.

To exploit the synthetic promoters for strain engineering, the synthetic promoter library was used to enhance the citric acid efflux through overexpression of the critical citric acid exporter gene *cexA*. The *cexA* gene was amplified with the primers of cexA-F and cexA-R, then cloned into the backbone of the corresponding synthetic promoters reporting plasmids, using the ClonExpress™ one-step cloning kit (Vazyme, C113), resulting in pXM10-pXM26, respectively (Table S2). These plasmids were used as the templates to amplify the donor DNAs containing the *cexA*-P2A-*mCherry-pyrG* expression cassettes driven by different synthetic promoters with different UAS elements (Table S5).

A. niger strains construction

The strains used in this study are listed in Table S1. The standard protocol of *A. niger* genome editing using the CRISPR/Cas9 system-based 5 S rRNA was performed as previously described [4, 11, 37]. To construct the reporting strains of the synthetic promoters, the donor DNA fragments containing *mCherry-pyrG* reporting cassettes driven by synthetic promoters were integrated into the genome locus of α-glucosidase encoding gene (*agdA*) to avoid the influence of the genomic context, resulting in the reported strains YT1-YT33, respectively. The DNA transformation into the *A. niger* D353.8 protoplasts was conducted by the PEG-mediated DNA transformation approach following the previously reported protocol [37]. The protoplasts were prepared in the protoplast lysing buffer with the Yatalase Enzyme (Takara, Cat#T017) and washed with the STC buffer [37]. Then, 2 μg donor DNA fragments were co-transformed into the protoplasts in the TC buffer [37] with 25 uL 25% PEG-6000 together with the sgRNA targeting constructs AgdA-sgRNA1, AgdA-sgRNA2, and Cas9 expression cassette amplified by the primers of Ptef-F and Ttef-R.

The transformants with fluorescence were selected after detection under the Tanon 5200 Multi fluorescence image system (Tanon, Tianjin, China). After the subculture, the genomic DNA of selected fluorescent transformants was extracted using a Genomic DNA extract kit (TIANGEN Biotech., Cat#DP305) according to the manufacturer's handbook (https://en.tiangen.com/-content/details_43_4227.html). Then, the genomic DNAs were verified by diagnostic PCR with the primers of agdA-g-F and mCherry-R and DNA sequencing analysis. Copy

number analysis was conducted with quantitative PCR (qPCR) Lightcycler 96 (Roche) using ChamQ Universal SYBR qPCR Master Mix (Vazyme) according to the manufacturer's instructions. The qPCR signal of *mCherry* was normalized to the *gpdA* gene as a reference. The qPCR primers are listed in Table S4. The correct single-integration isolates were chosen for further fluorescence detection.

Similarly, citric acid-producing engineered strains XMD9-XMD26 (Table S1) were also constructed using the same tactics. The differences were the donor DNAs containing *cexA* expression cassette, amplified with the primers of MH-agdA-sgRNA1-F and MH-agdA-sgRNA1-R, using pYDD2, pXM10-pXMD26 as the templates (Table S2), respectively. After the subculture, the genomic DNAs of selected transformants were extracted and verified via diagnostic PCR and sequencing analysis with the primers of agdA-g-F and cex-R. The correct isolates were chosen for further citric acid fermentation.

Flow cytometry analysis

The fluorescence of the conidia of the reporting strains was quantitatively determined through flow cytometry, as described in the previous study [11]. Briefly, *A. niger* strains were cultivated on CM plates for five days. Then, conidia were collected and diluted in Phosphate Buffer Solution (PBS) and filtered through four-layer lens cleaning paper before flow cytometry analysis using a BD Fortessa X-20 cell sorter (Becton, Dickinson and Company, Piscataway, NJ 08855 – 1327, USA). A green (561 nm) laser and a 610 nm filter were used for mCherry fluorescence determination. The forward scatter (FSC) voltage, side scatter (SSC), and PE-CF 594 were set as 50, 170, and 489, respectively. Minor gating was performed on data to exclude apparent errors, such as dust particles, cell clusters, and conidia aggregates. 100, 000 cells of each sample were recorded and used for mCherry fluorescence and forward scatter (FSC). Flow cytometry results were analyzed with FlowJo software (Becton, Dickinson and Company, Piscataway, NJ 08855-1327, USA). The *t*-test was used for statistical analysis of the data.

Citric acid fermentation and detection

To test the application of synthetic promoters on citric acid production, citric acid fermentation was carried out using the liquefied corn media as described in previous studies [11, 38]. Spores with the final concentration of 1×10^5 spores/ml were inoculated in 20 mL liquefied corn media at 34 °C and 220 rpm for 120 h. The weight of the shake flasks was measured before and after the citric acid fermentation to eliminate measurement errors caused by evaporation. For citric acid production in the 5 L bioreactor with stirring paddle devices, the same fermentation parameters were utilized for 120 h, with the aeration rate coupled to the dissolved oxygen concentration of 40–60% [11].

For extracellular citric acid detection, supernatants were separated from cultures by filter paper after fermentation. Total acids were titrated using 142.9 mM NaOH with 20 µL 0.1% phenolphthalein as pH indicator. After titration, supernatants were diluted in sterile distilled water depending on the estimated total acid. Samples were boiled for 15 min at 100 °C, centrifuged at 12,000 rpm for 5 min, and filtered through a 0.22 µm sterile filter membrane to collect the supernatant. Extracellular organic acids were detected by Prominence UFLC equipped with a UV detector (Shimadzu, Kyoto, Japan) and a Bio-Rad Aminex HPX-87 H column (300 × 7.8 mm) according to the procedure described previously [11, 38].

Results

Identification of UAS elements from the promoter regions of *Aspergillus* amylatic genes

Since the 12 tandem repeats of region III of P*AoagdA* were reported to improve the native promoter strength in *A. oryzae* [23], we supposed that Region III might consist of one or more transcription factor binding sites (TFBSs) and function as a promoter-enhancing sequence. Inspired by this hypothesis, we predicted the Region III-like sequences in three highly expressed amylolytic genes encoding amylase (*amyA*), α-glucosidase (*agdA*), and glucoamylase (*glaA*), according to the *A. niger* transcriptomic profiling under glucose gradients [39] and the multiple sequence alignments of their promoters sequences in different *Aspergilli* species, including *A. niger*, *A. oryzae*, *A. nidulans*, *Aspergillus pseudonomiae*, *Aspergillus brasiliensis*, and *Aspergillus tubingensis* (Fig. 1A). Based on the reported Region III sequence of P*agdA* in *A. oryzae* [34], several conserved Region III-like sequences were predicted in the *amyA*, *agdA*, and *glaA* promoters of various *Aspergilli*. The Region IIIa sequences have been indicated in all three promoters, while the Region IIIb sequences were only found in the P*agdA* and P*glaA* promoters. The Region IIIa sequences and their flanking sequences were more diverse than the Region IIIb sequences (Fig. 1A). Consequently, the 70-bp or 80-bp DNA sequences containing the Region III-like sequences of the P*amyA*, P*agdA*, and P*glaA* promoters were considered putative UAS elements.

To investigate the function of the UAS element candidates, they were integrated into the core element of the P*gpdA* promoter to construct three synthetic promoters: UASa-P*gpdA*, UASb-P*gpdA*, and UASc-P*gpdA*, respectively (Fig. 1 and Figure S1). Subsequently, a fluorescent-auxotrophic double-check workflow was employed to evaluate the synthetic promoter activity by combining the CRISPR/Cas9 system with flow cytometry (Fig. 1B). To eliminate the impact of the reporting gene integration

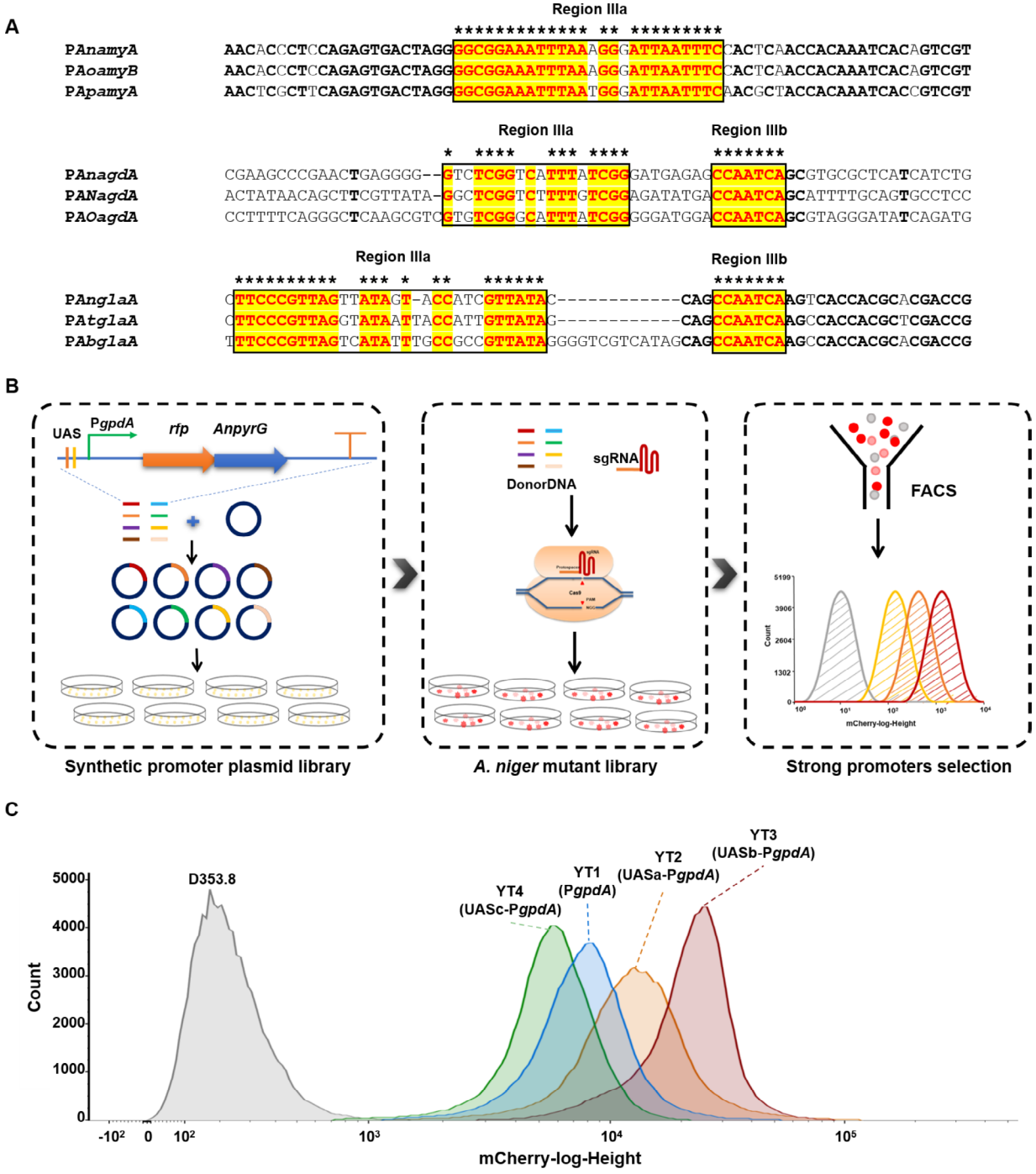

Fig. 1 UAS elements prediction and characterization in *A. niger*. (**A**) Multiple sequence alignment of potential Region III sequences of highly expressed amylolytic enzymes protomers from various *Aspergilli spp*. The GenBank accession numbers of the selected genes included *amyA* of *A. niger* CBS 513.88 (*AnamyA*, An05g02100), *A. oryzae* RIB40 (*AoamyB*, AO090120000196), and *Aspergillus pseudonomiae* (*ApamyA*, Asppsen1_70912); *agdA* of *A. niger* CBS 513.88 (*AnagdA*, An04g06920), *A. nidulans* FGSC A4 (*ANagdA*, AN2017) and *A. oryzae* RIB40 (*AoagdA*, AO090003001209); and *glaA* of *A. niger* CBS 513.88 (*AnglaA*, An03g06550), *Aspergillus brasiliensis* CBS 101,740 (*AbglaA*, KV878703) and *Aspergillus tubingensis* CBS 134.48 (*AtglaA*, KV878178). The predicted conserved sequences of Region IIIa and IIIb were highlighted in red fonts with a yellow background and black asterisks in the black boxes. The other conserved sequences in each promoter region were also shown in bold black fonts. (**B**) The UAS elements characterization and evaluation workflow combined the efficient CRISPR/Cas9 genetic manipulation system, the fluorescent protein-selection marker fused indicator, and flow cytometry-based analysis. (**C**) The fluorescence analysis of the reporting strains expressing *mCherry-pyrG* controlled by the synthetic promoters with different UAS elements. The 100,000 spores were analyzed by flow cytometry. *A. niger* YT1 with the promoter of P*gpdA* was used as a positive control, while the parent strain D353.8 was used as a negative control. *A. niger* YT2, YT3, and YT4 represented the fluorescence reporting strains for synthetic promoters with UASa, UASb, and UASc, respectively

locus, the fused protein *mCherry-PyrG* expression cassettes under the control of synthetic promoters were precisely integrated into the genomic locus of the *agdA* gene. Flow cytometry determined the reporter mutants' fluorescence intensity to reflect the promoter activity (Fig. 1B). As shown in Fig. 1C and Figure S1, the *mCherry-pyrG* reporting strain YT3, under the control of UASb-P*gpdA*, exhibited the highest fluorescence intensity with a 1.3-fold increase compared with the P*gpdA* promoter. Similarly, the fluorescence of the reporting strain YT2 with UASa-P*gpdA* also reached up to 1.2-fold that of the P*gpdA* promoter. In contrast, adding the UASc element from the P*glaA* promoter reduced fluorescence. These results indicated that the 70-bp sequences within Region III of the P*amyA* and P*agdA* promoters could function as the UAS elements to enhance promoter activity.

Modulating synthetic promoter strength by varying tandem UAS elements

To investigate the effect of tandem UAS elements on promoter activity, we generated a series of tandem UASa and UASb elements through PCR amplifications with overlapping primers (Table S4) and constructed synthetic promoters by fusing them to the P*gpdA* promoter (Figure S2). To avoid the influence of integration site, all the promoter reporting cassettes were targeted to the *adgA* gene locus, owing to its favorable transcriptional accessibility. For each construct, four transformants with fluorescence were randomly selected and verified by diagnostic PCR, qPCR and DNA sequencing confirmation (Figure S3 and Table S5). It demonstrated that all these selected isolates, containing repeats of the UASa and UASb elements, were confirmed with a single copy of *mCherry-pyrG* fusion inserted at the *agdA* locus (Figure S3). The expression of *mCherry-pyrG* under the synthetic promoter variants was evaluated by fluorescence using flow cytometry of conidia, which was consistent with the fluorescence of mycelial pellets of each strain detected by microscopes (Fig. 2 and Figure S4). The result demonstrated that increasing the copies of UASa and UASb led to a gradual and significant improvement in synthetic promoter strength. In particular, the fluorescence intensity of the mutants with the synthetic promoters $(UASa)_6$-P*gpdA* and $(UASb)_5$-P*gpdA*, containing six copies of UASa and five copies of UASb, peaked at 3.5-fold and 5.4-fold that of the positive control with the P*gpdA* promoter, respectively. However, increasing the copy number of UASa and UASb could not further enhance the fluorescence intensity of the reporting strains. For example, when the copies of UASa and UASb reached eleven, the mCherry fluorescence intensity of the reporting strains leveled to 2.4-fold and 3.4-fold, like that of the three-copy constructs. Additionally, the UASb element showed remarkable improvement in promoter activity for the same copy number as UASa. These data validated that the UASa and UASb elements play a crucial role in promoter strength, and their tandem arrangement provided a strategy to modulate the promoter activity.

To further evaluate modular compatibility between the UAS elements and different core promoter elements, we selected the UASb element to design different synthetic promoters fused with the core elements of the P*pkiA* and P*citA* promoters (Fig. 3). Similarly, the synthetic promoter reporting cassettes were integrated into the *adgA* gene locus, and the resulting strains were verified by genomic PCR and DNA sequencing (Figure S5 and Table S5). The effect of the UASb element on transcription efficiency driven by synthetic promoters was evaluated based on the fluorescence intensity of the *mcherry-pyrG* reporting strains in conidia and mycelial pellets (Fig. 3 and Figure S5). Compared with the corresponding original promoters P*pkiA*, P*citA*, and P*gpdA*, the addition of a single copy of UASb resulted in considerable improvement in promoter activity, with 2.9-fold, 1.9-fold, and 1.3-fold increases, respectively (Figs. 2B and 3). To identify combinations that maximize promoter activity, we constructed synthetic promoters with multiple repeats of the UASb element fused to the core elements of P*pkiA* and P*citA* (Figure S5). The expression of *mCherry-pyrG* under the synthetic promoter variants was evaluated by fluorescence using flow cytometry of conidia and microscopic images of mycelial pellets (Figure S5). The results demonstrated that increasing the number of UASb repeats gradually enhanced the promoter activity of the P*pkiA* and P*citA* promoters, similar to the effect observed with the P*gpdA* promoter. Two copies of the UASb element further enhanced the transcription level of the *mCherry-pyrG* gene up to 4.9-fold, 2.7-fold, and 1.9-fold, compared to the original promoters P*pkiA*, P*citA*, and P*gpdA*, respectively (Figs. 2B and 3). Furthermore, the addition of four copies of the UASb element into the core elements of P*pkiA*, P*citA*, and P*gpdA* achieved up to a 7.3-fold, 3.8-fold, and 4.8-fold increase in promoter strength, respectively (Figs. 2B and 3). These results indicated that the UAS elements were functionally robust and highly efficient in *A. niger*. It established a series of strong synthetic promoters by assembling the UAS element in a hybrid manner into different promoter core elements.

Establishing synthetic promoters by hybrid tandem UAS elements

To evaluate whether hybrid UAS elements could enhance promoter strength in *A. niger*, the UASa and UASb elements were assembled in tandem (Fig. 4 and Figure S6-7). The results demonstrated that the promoter activities were significantly affected by the arrangement order of the UAS elements (Figure S6). Additionally, the synthetic

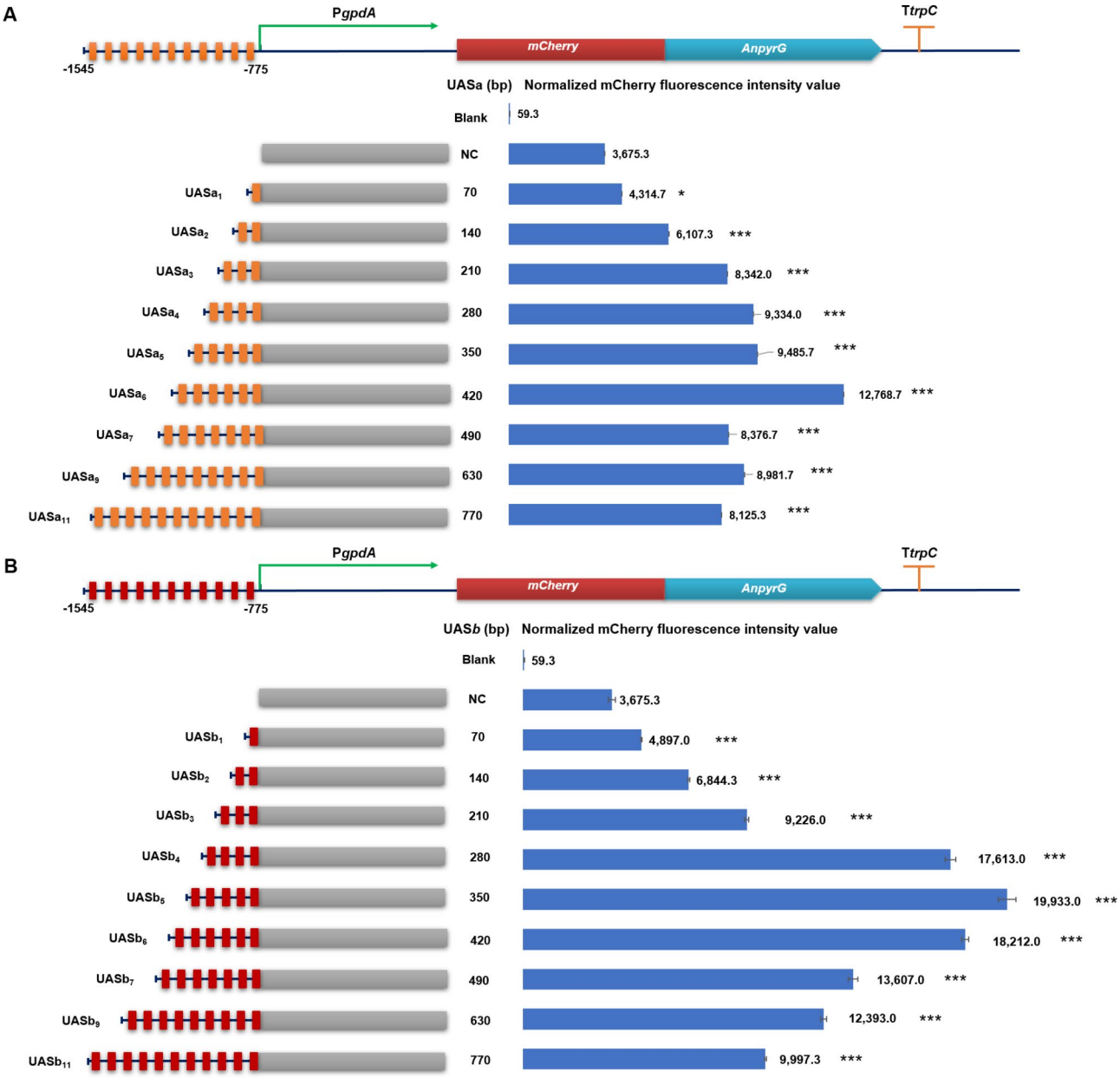

Fig. 2 Characterization of the effect of copy number of UASa and UASb elements on the transcription activity of the synthetic promoters. Schematic diagrams and fluorescence analyses of the constructs expressing *mCherry-pyrG* controlled by the synthetic promoters with different copies of UASa (**A**) and UASb (**B**) were depicted. The overlap extension PCR amplified the copies of UAS elements and fused the core elements of the P*gpdA* promoter. UASa and UASb were represented as orange bars and red bars, respectively. The P*gpdA* promoter was displayed as grey bars. The mean mCherry fluorescence intensity of each construct was shown as blue bars. Results are the mean of three replicates, and error bars indicate standard deviations ($n = 3$). Pairwise Student's *t-tests* were conducted between the mutants with synthetic promoters and the P*gpdA* promoter. *p* values were indicated as asterisks (< 0.05, *; <0.001, ***)

promoter reporting cassettes were integrated into the *adgA* gene locus, generating the strains YT29 to YT35, which were verified through genomic PCR and DNA sequencing (Figure S7 and Table S5). The fluorescence intensity of the *mCherry-pyrG* gene expression of the conidia and mycelial pellets under the control of a synthetic promoter containing UASb-UASa was detected (Fig. 4 and Figure S7). It demonstrated that the activity of these synthetic promoters with the UASb-UASa elements was higher than the ones with the UASa-UASb elements, both of which had increases of 2.6-fold and 2.0-fold compared to the P*gpdA* promoter, respectively (Fig. 4). As the copies of the hybrid UAS elements increased, the activity of the synthetic promoters improved. Notably, two copies of hybrid UASa-UASb and UASb-UASa led to a significant increase in promoter strength, reaching up to

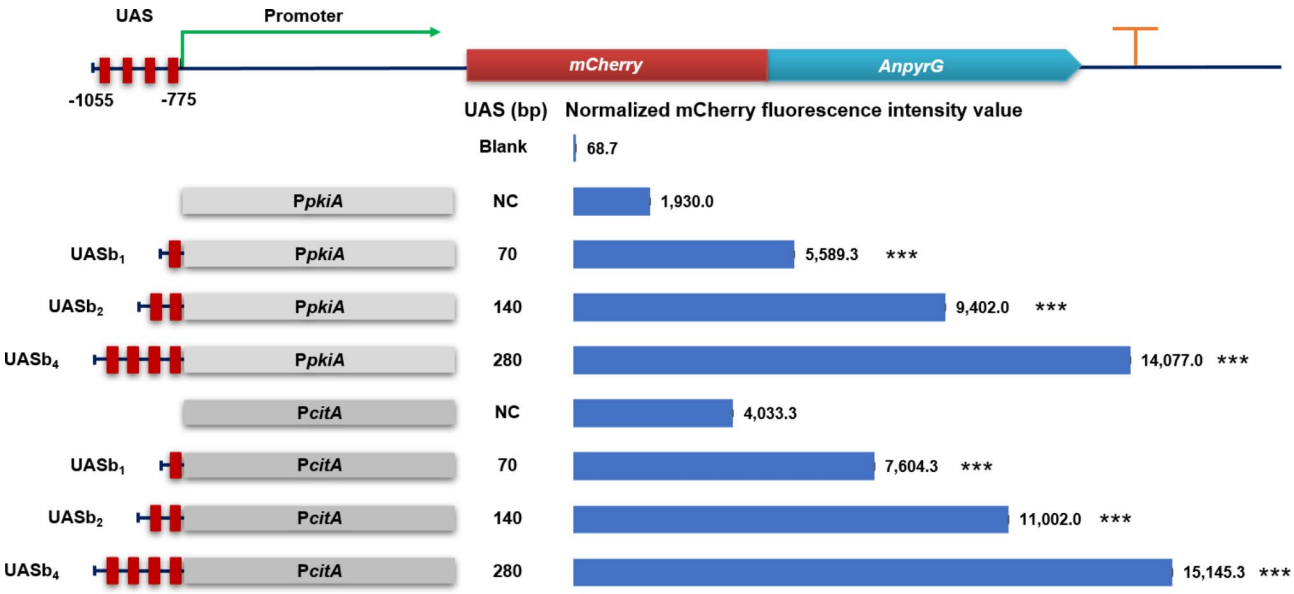

Fig. 3 Effect of the UASb element on synthetic promoters with different core promoter elements. One, two, and four copies of the UASb element were fused into the core elements of the P*pkiA* and P*citA* promoters to test the compatibility between the UAS elements and the core promoter elements. UASb was represented as red bars. The core elements of the P*pkiA* and P*citA* promoters were displayed as light grey and dark grey bars, respectively. The mean mCherry fluorescence intensity of each construct was shown as blue bars. Results are the mean of three replicates, and error bars indicate standard deviations ($n = 3$). Pairwise Student's *t-tests* were conducted between synthetic promoters and the corresponding parent promoter. *p* values were displayed as asterisks (< 0.001, ***)

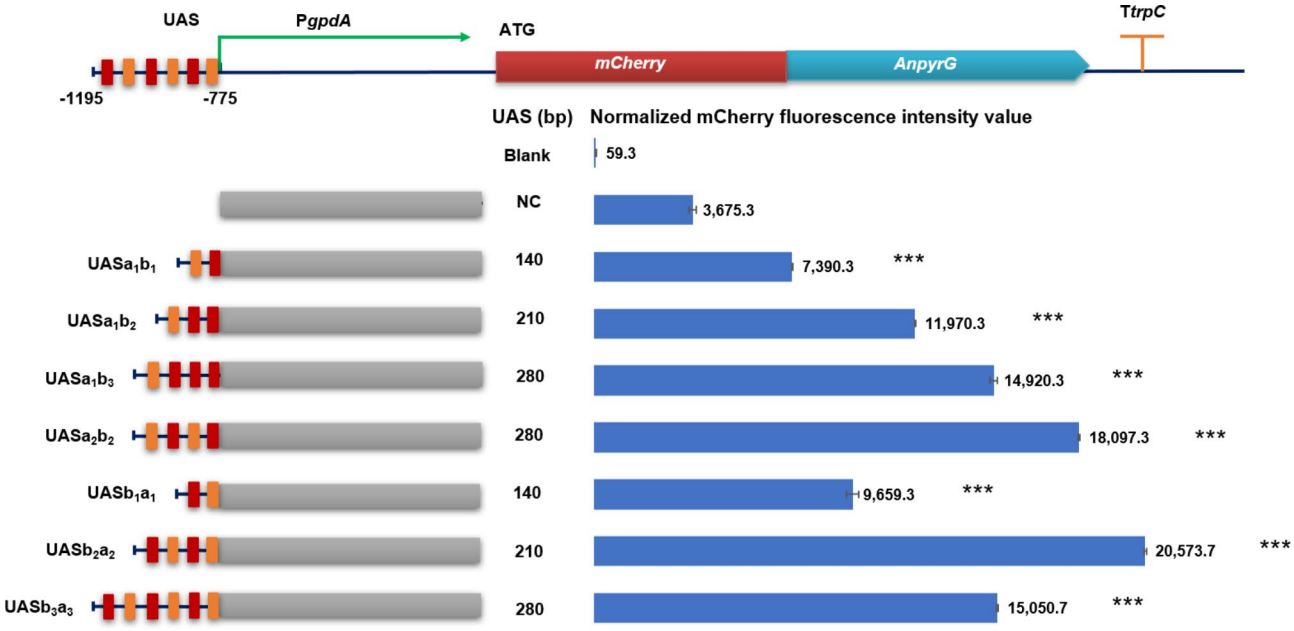

Fig. 4 Characterization of synthetic promoters with the hybrid tandem UASa and UASb elements. The synthetic promoters with the hybrid UAS elements of UASa and UASb were constructed using different UAS arrangements. Fluorescence analysis of constructs expressing *mCherry-pyrG* controlled by synthetic promoters was conducted using flow cytometry. UASa and UASb were represented as orange bars and red bars, respectively. The core elements of the P*gpdA* promoters were displayed as grey bars. The mean mCherry fluorescence intensity of each construct was shown as blue bars. Results are the mean of three replicates, and error bars indicate standard deviations ($n = 3$). Pairwise Student's *t-tests* were conducted between synthetic promoters and the P*gpdA* promoter. *p* values were shown as asterisks (< 0.001, ***)

4.9-fold and 5.6-fold of the P*gpdA* promoter, respectively (Fig. 4). The strength of synthetic promoter with (UASb-UASa)$_2$ exceeded that of all other synthetic promoters. To summarize, we have established a library of synthetic promoters with various activities using combinations of the identified functional UAS elements.

Application of the synthetic promoter library for citrate efflux optimization significantly improved citric acid production in *A. niger*

To assess the utility of the established synthetic promoter library in an industrially relevant application, we conducted promoter engineering of the citric acid exporter encoding gene *cexA*, which played an essential role in citric acid efflux [40]. With the assistance of the highly efficient CRISPR/Cas9 genome editing toolbox [4], donor DNAs containing the *cexA* expression cassettes driven by the synthetic promoter library with varying promoter strengths were successfully integrated into the *agdA* gene locus in *A. niger* (Fig. 5 and Figure S8). Following verification by genomic PCR and sequencing analysis, correctly integrated isolates with different promoters were selected for citric acid fermentation in shake flasks (Figure S8). The UAS elements in each synthetic promoter and their corresponding DNA sequences are showed in Table S1 and Table S5, respectively. As expected, all the *cexA* overexpressing strains under the control of synthetic promoters with extra tandem UAS elements achieved significantly higher citric acid production than the positive control XMD9 with the constitutive strong promoter P*gpdA* (Fig. 5B). Notably, the strains with synthetic promoters containing tandem identical UAS elements, such as XMD12 with (UASa)$_5$-P*gpdA* and XMD17 with (UASb)$_4$-P*gpdA*, exhibited high citric acid production of 132.3 ± 0.2 g/L and 141.7 ± 1.3 g/L, respectively, which were 1.4-fold and 1.5-fold that of XMD9 with the P*gpdA* promoter. All strains with tandem hybrid UAS elements achieved a nearly 1.5-fold increase in citric acid titer compared to the positive control XMD9. For instance, the citric acid production of the stain XMD25 with the (UASa)$_1$-(UASb)$_2$-P*gpdA* promoter reached up to 145.3 ± 3.8 g/L, which was 1.6-fold that of XMD9 with the P*gpdA* promoter. These data indicated that the synthetic promoter library enables fine-tuned metabolic pathway optimization, which is essential for achieving industrially feasible production levels.

Discussion

The filamentous fungus *A. niger* is a leading industrial cell factory to produce organic acids and enzymes. Promoters are crucial to optimize gene expressions for synthetic biology and strain engineering. However, due to a knowledge gap in fully understanding native promoters and their architectures, there is a shortage of strong promoters available in *A. niger*. To overcome these limitations, we identified two functional UAS elements, UASa and UASb, and constructed a synthetic promoter library with vigorous intensity and an extensive range. This library facilitated the fine-tuned gene expression of the *cexA* gene and improved citric acid productivity.

In fungi, many yeast promoters have been well-characterized [22, 31], and many UAS elements have been identified in the yeast constitutive promoters. These identified UAS elements have been exploited to design hybrid promoters and stimulate transcription initiation with higher efficiency in yeast [23, 24, 27, 41]. By contrast, only a few such UAS elements were identified in filamentous fungi. For instance, a 200-bp DNA fragment was identified in the most potent inducible promoter, P*cbh1* of *Trichoderma reesei*, which enhanced the promoter strength when fused to a constitutive promoter, P*cdna1* [42]. Few DNA sequences in strong inducible promoters were found to improve their native original promoters' activity, such as a CCAAT-containing sequence in the P*glaA* promoter of *A. niger* T21 [32] and a Region III sequence in the P*agdA* promoter of *A. oryzae* [34]. To identify more functional promoter-enhancing sequences, here, we predicted the potential UAS elements in three highly expressed amylolytic genes *agdA*, *amyA*, and *glaA* in *A. niger* (Fig. 1). Among them, UASa from the P*agdA* promoter and UASb from the P*amyA* promoter were identified to enhance the promoter activities. Remarkably, UASb improved the activity of the P*gpdA* promoter by 33% (Fig. 1C). Moreover, the UASb element could work well after truncation to a 30-bp conserved sequence. Overall, these two identified UAS elements can confer more efficient promoter activity. In addition, we also surprisingly found that the UASc of the P*glaA* promoter, with the conservated motifs of the CCAAT-containing sequence in P*AnglaA* of A. *niger* T21, didn't show any improved effect on the P*gpdA* promoter activity (Fig. 1C), which was not consistent with the previous report [32]. This inconsistency might be caused by random mutations in Region III of UASc spontaneously generated when the UASc sequence was synthesized and constructed in *E. coli* (Figure S9).

Due to the distinctive functional feature of UAS elements, many researchers have invested efforts in enhancing promoter activity through synthetic hybrid promoter engineering in yeast [7, 22, 23, 27, 30]. Synthetic hybrid promoters have been designed using tandem UAS elements, assembling different UAS elements, or replacing core elements [27]. This study established a synthetic hybrid promoter library with high activities and a wide range by making these two identified UAS elements. We observed that increasing the number of UAS element repeats enhanced promoter strength, corroborating previous studies on UAS1B in *Y. lipolytica* [23] or the BS

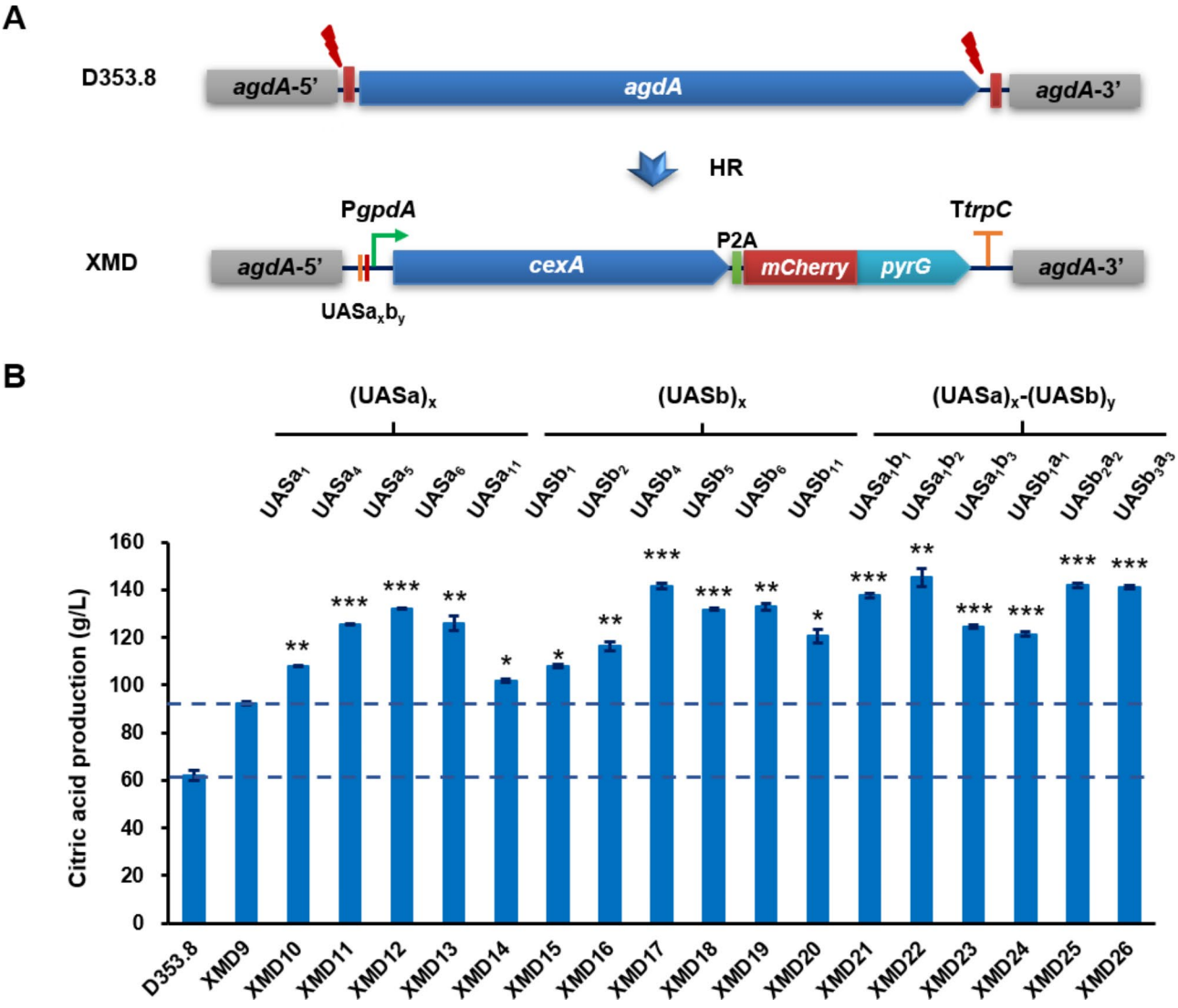

Fig. 5 Citric acid production of *A. niger* strains expressing *cexA* under the control of synthetic promoters. (**A**) Schematic diagram of the construction of the *cexA* expressing mutants. The donor DNAs containing *CexA*-expressing cassettes with synthetic promoters were integrated into the genomic locus of the *agdA* gene at DNA double-strand breaks (DSBs) generated by Cas9 under the guide of two sgRNA (agdA-sgRNA1 and agdA-sgRNA2). (**B**) Citric acid production of the *cexA* expressing mutants. The spores with 1×10^5/ml concentration were inoculated in 20 ml citrate fermentation media and incubated at 34 °C for 120 h. The extracellular citric acid titer was determined by HPLC. *A. niger* XMD9 with *cexA* expression cassette under the control of the P*gpdA* promoter and was used as a positive control. The UAS elements used in each strain were shown above each column. Specifically, XMD10: UASa$_1$, XMD11: UASa$_4$, XMD12: UASa$_5$, XMD13: UASa$_6$, XMD14: UASa$_{11}$, XMD15: UASb$_1$, XMD16: UASb$_2$, XMD17: UASb$_4$, XMD18: UASb$_5$, XMD19: UASb$_6$, XMD20: UASb$_{11}$, XMD21: UASa$_1$b$_1$, XMD22: UASa$_1$b$_2$, XMD23: UASa$_1$b$_3$, XMD24: UASb$_1$a$_1$, XMD25: UASb$_2$a$_2$, XMD26: UASb$_3$a$_3$. Results are the mean of three replicates, and error bars indicate standard deviations ($n = 3$). Pairwise Student's *t-test* was conducted between the *cexA* expressing mutants with synthetic promoters and the positive control XMD9. *p* values were shown as asterisks (< 0.05, *; <0.01, **; <0.001, ***)

motifs in the SES system [18]. However, the synthetic promoter activity declined beyond a certain number of repeats (Fig. 2). There appears to be a critical threshold for UAS repeats, such as 6 copies for UASa and 5 copies for UASb. Notably, six copies of UASamyA and five copies of UASagdA conferred significant improvements in the transcription efficiency of synthetic promoters, up to 3.5-fold and 5.4-fold that of the strong P*gpdA* promoter (Fig. 2). Similar phenomena have been reported in other studies. For instance, Cox et al. found that a palindromic cAMP response element (CRE) functions as a UAS element for constructing synthetic promoters [43]. The optimal number of tandem-repeated CREs was 9 or 12, but promoter strength significantly declined when the CRE repeats were increased to 15 or 18 [43]. Based on the observed saturation phenomena of the UAS elements, we speculate that a certain number of UAS repeats could facilitate the binding of transcription activators and improve the recruitment of transcription factors (TFs) and RNA polymerase; however, further the

increased UAS repeats may change the DNA accessibility and possibly affect the localization of transcription activators and RNA polymerases, which hinders their effective recruitment. The underlying reasons behind this interesting phenomenon could be further discovered by structure analysis of the complex involved in transcription initiation.

Compatibility of UAS elements with different core elements is crucial for designing synthetic promoters. Zhao et al. [23] demonstrated that the UAS1B element exhibited vigorous activity when fused to various core promoter elements in *Y. lipolytica*, including LEU, TEF, PAT1, POX2, and EXP. In this study, we showed that the UAS elements also displayed good compatibility with the core elements of the P*pkiA* and P*citA* promoters in *A. niger*. For instance, four copies of the UASagdA element achieved up to 7.3-fold and 3.8-fold increases in the strength of the P*pkiA* and P*citA* promoters, respectively (Fig. 3). This compatibility highlights the potential of UAS elements to broaden the design range of artificial promoters, facilitating more versatile and effective transcriptional regulation.

In addition, we revealed that the UAS elements showed good functional modularity and that tandem hybrid UAS elements can collaboratively enhance promoter strength. Notably, two copies of UASagdA-UASamyA dramatically increased the promoter strength up to 5.6-fold that of the P*gpdA* promoter. This functional modularity of the UAS elements has been verified in yeast UAS elements, such as UAS1 and UAS2, from the promoters Pro-Y13 and Pro-Y14 in *O. polymorpha* [29]. The Phy4 promoter with a hybrid tandem fusion of $UAS1^{Y13}+UAS2^{Y13}$ and $UAS1^{Y14}+UAS2^{Y14}$ showed a 2-fold increase in activity compared to the original promoter. The strong modularity of the UAS elements enables the design of shorter but more powerful synthetic promoters.

For the application testbed, the *cexA* overexpression driven by this synthetic promoter library led to much higher citric acid production than that of the P*gpdAg* promoter. Among the synthetic promoters, the highest citric acid production was achieved at 145.3 g/L by fusing with hybrid tandem UAS elements (Fig. 5). These obtained synthetic promoters, exhibiting strength far surpassing that of the previously reported most potent promoter [11], P*gpdA*, provided additional options for strong gene regulatory elements in *A. niger* strain engineering. The activation effect of the UAS elements on promoter strength involves some specific transcription activators [22, 44]. In the future, more efforts should be put into the screening of UAS interacting transcription activators to achieve a synthetic gene regulatory system with more commonality, more robust activity, and a broader range of gene transcription levels to achieve high-level production of organic acids and enzymes by this important cell factory *A. niger*.

Conclusion

In this study, two functional UAS elements, UASamyA and UASagdA, were identified from the promoter of highly expressed genes in *A. niger*. Based on these UAS elements, we created a synthetic promoter library with high activities and a broad range by assembling UAS elements with the reported most potent P*gpdA* promoter. We also demonstrated that these UAS elements were well-compatible with the core elements of different promoters. This synthetic promoter library was successfully applied to optimize citric acid-producing strains, resulting in significantly higher citric acid production in *A. niger*. In summary, the findings in this study lay the groundwork for developing more efficient synthetic promoter systems and expanding the promoter engineering toolboxes in fungal cell factories.

Supplementary Information

The online version contains supplementary material available at https://doi.org/10.1186/s12934-025-02642-y.

Additional files 1: **Figure S1**. Flow cytometry scatter plots of the reporting mutants with the synthetic promoters containing different UAS elements; **Figure S2**. Construction of tandem UASa and UASb elements by PCR amplification; **Figure S3**. Constructs expressing *mCherry-pyrG* controlled by the synthetic promoters with the UASa and UASb repeats; **Figure S4**. Representative fluorescence images in mycelial pellets of the constructs expressing *mCherry-pyrG* controlled by synthetic promoters with the UASa and UASb elements; **Figure S5**. Constructs expressing *mCherry-pyrG* controlled by the synthetic promoters with the UASb repeats and different core promoter elements of P*pkiA* and P*citA*; **Figure S6**. Construction of hybrid UASa and UASb elements by PCR amplification; **Figure S7**. Constructs expressing *mCherry-pyrG* controlled by the synthetic promoters with the hybrid UASa and UASb elements; **Figure S8**. Constructs overexpressing *cexA* controlled by the synthetic promoters with the UASa and UASb elements; **Figure S9**. The multiple sequence alignment of DNA sequences of the synthesized UASc isolates; **Table S1**. Strains used in the study; **Table S2**. Plasmids used in this study; **Table S3**. Protospacers used in this study; **Table S4**. Primers used in this study; **Table S5**. DNA sequences of the UAS elements used in this study.

Acknowledgements

This work was supported by the Tianjin Institute of Industrial Biotechnology, Chinese Academy of Sciences.

Author contributions

X.Z., P.Z., and J.S. conceived the study. X.Z. designed the experiments. Y.G., M.C., Yd. L. and Y.D. performed the experiments. Y. L. involved in genome verification of synthetic promoter reporting strains. X.Z. drafted and revised the manuscript. Y.G. prepared Figs. 1, 2, 3, 4, 5 and 6. P.Z. and J.S. revised the manuscript. All authors approved the manuscript.

Funding

The work was supported by the National Natural Science Foundation of China (32070082), the Key R&D Program of Shandong Province (2022SFC0101), the Tianjin Synthetic Biotechnology Innovation Capacity Improvement Project (TSBICIP-PTJS-003 and TSBI-CIP-IJCP-003).

Data availability

No datasets were generated or analysed during the current study.

Declarations

Ethics approval and consent to participate
Not applicable.

Consent for publication
Not applicable.

Competing interests
The authors declare no competing interests.

Received: 18 October 2024 / Accepted: 2 January 2025
Published online: 15 January 2025

References

1. Meyer V, Wu B, Ram AF. Aspergillus as a multi-purpose cell factory: current status and perspectives. Biotechnol Lett. 2011;33:469–76.
2. Tong Z, Zheng X, Tong Y, Shi YC, Sun J. Systems metabolic engineering for citric acid production by Aspergillus Niger in the post-genomic era. Microb Cell Fact. 2019;18:28.
3. Meyer V, Cairns T, Barthel L, King R, Kunz P, Schmideder S, Muller H, Briesen H, Dinius A, Krull R. Understanding and controlling filamentous growth of fungal cell factories: novel tools and opportunities for targeted morphology engineering. Fungal Biol Biotechnol. 2021;8:8.
4. Zheng X, Zheng P, Zhang K, Cairns TC, Meyer V, Sun J, Ma Y. 5S rRNA promoter for Guide RNA expression enabled highly efficient CRISPR/Cas9 genome editing in Aspergillus Niger. ACS Synth Biol. 2019;8:1568–74.
5. Rozhkova AM, Kislitsin VY. CRISPR/Cas Genome Editing in Filamentous Fungi. Biochem (Mosc). 2021;86:S120–39.
6. Zheng X, Zheng P, Sun J. CRISPR/Cas-based genome editing in Aspergillus Niger. Sheng Wu Gong Cheng Xue Bao. 2021;37:980–90.
7. Blazeck J, Alper HS. Promoter engineering: recent advances in controlling transcription at the most fundamental level. Biotechnol J. 2013;8:46–58.
8. Blumhoff M, Steiger MG, Marx H, Mattanovich D, Sauer M. Six novel constitutive promoters for metabolic engineering of Aspergillus Niger. Appl Microbiol Biotechnol. 2013;97:259–67.
9. Dave K, Punekar NS. Utility of aspergillus Niger citrate synthase promoter for heterologous expression. J Biotechnol. 2011;155:173–7.
10. Xue X, Bi F, Liu B, Li J, Zhang L, Zhang J, Gao Q, Wang D. Improving citric acid production of an industrial aspergillus Niger CGMCC 10142: identification and overexpression of a high-affinity glucose transporter with different promoters. Microb Cell Fact. 2021;20:168.
11. Lu Y, Zheng X, Wang Y, Zhang L, Wang L, Lei Y, Zhang T, Zheng P, Sun J. Evaluation of Aspergillus Niger six constitutive strong promoters by fluorescent-auxotrophic selection coupled with Flow Cytometry: a case for citric acid production. J Fungi (Basel) 2022, 8.
12. Potter CJ, Tasic B, Russler EV, Liang L, Luo L. The Q system: a repressible binary system for transgene expression, lineage tracing, and mosaic analysis. Cell. 2010;141:536–48.
13. Riabinina O, Potter CJ. The Q-System: a versatile expression system for Drosophila. Methods Mol Biol. 2016;1478:53–78.
14. Persad R, Reuter DN, Dice LT, Nguyen MA, Rigoulot SB, Layton JS, Schmid MJ, Poindexter MR, Occhialini A, Stewart CN Jr. Lenaghan SC: the Q-System as a Synthetic Transcriptional Regulator in plants. Front Plant Sci. 2020;11:245.
15. Fölsz O, Lin CC, Task D, Riabinina O, Potter CJ. The Q-system: a versatile repressible binary expression system. Methods Mol Biol. 2022;2540:35–78.
16. Meyer V, Wanka F, van Gent J, Arentshorst M, van den Hondel CA, Ram AF. Fungal gene expression on demand: an inducible, tunable, and metabolism-independent expression system for Aspergillus Niger. Appl Environ Microbiol. 2011;77:2975–83.
17. Wanka F, Cairns T, Boecker S, Berens C, Happel A, Zheng X, Sun J, Krappmann S, Meyer V. Tet-on, or Tet-off, that is the question: Advanced conditional gene expression in Aspergillus. Fungal Genet Biol. 2016;89:72–83.
18. Rantasalo A, Landowski CP, Kuivanen J, Korppoo A, Reuter L, Koivistoinen O, Valkonen M, Penttilä M, Jäntti J, Mojzita D. A universal gene expression system for fungi. Nucleic Acids Res. 2018;46:e111.
19. Fowler T, Berka RM, Ward M. Regulation of the glaA gene of Aspergillus Niger. Curr Genet. 1990;18:537–45.
20. Ganzlin M, Rinas U. In-depth analysis of the Aspergillus Niger glucoamylase (glaA) promoter performance using high-throughput screening and controlled bioreactor cultivation techniques. J Biotechnol. 2008;135:266–71.
21. Wu N, Wu X, Zhang M, Zhang C, Xu Q. Metabolic engineering of aspergillus Niger for accelerated malic acid biosynthesis by improving NADPH availability. Biotechnol J. 2024;19:e2400014.
22. Cazier AP, Blazeck J. Advances in promoter engineering: novel applications and predefined transcriptional control. Biotechnol J. 2021;16:e2100239.
23. Zhao Y, Liu S, Lu Z, Zhao B, Wang S, Zhang C, Xiao D, Foo JL, Yu A. Hybrid promoter engineering strategies in Yarrowia Lipolytica: isoamyl alcohol production as a test study. Biotechnol Biofuels. 2021;14:149.
24. Blazeck J, Garg R, Reed B, Alper HS. Controlling promoter strength and regulation in Saccharomyces cerevisiae using synthetic hybrid promoters. Biotechnol Bioeng. 2012;109:2884–95.
25. Van Slyke C, Grayhack EJ. The essential transcription factor Reb1p interacts with the CLB2 UAS outside of the G2/M control region. Nucleic Acids Res. 2003;31:4597–607.
26. Rosenkrantz M, Kell CS, Pennell EA, Webster M, Devenish LJ. Distinct upstream activation regions for glucose-repressed and derepressed expression of the yeast citrate synthase gene CIT1. Curr Genet. 1994;25:185–95.
27. Li S, Ma L, Fu W, Su R, Zhao Y, Deng Y. Programmable synthetic upstream activating sequence Library for fine-tuning gene expression levels in Saccharomyces cerevisiae. ACS Synth Biol. 2022;11:1228–39.
28. Blazeck J, Reed B, Garg R, Gerstner R, Pan A, Agarwala V, Alper HS. Generalizing a hybrid synthetic promoter approach in Yarrowia Lipolytica. Appl Microbiol Biotechnol. 2013;97:3037–52.
29. Ye M, Gao J, Li J, Yu W, Bai F, Zhou YJ. Promoter engineering enables precise metabolic regulation towards efficient β-elemene production in Ogataea Polymorpha. Synth Syst Biotechnol. 2024;9:234–41.
30. Redden H, Alper HS. The development and characterization of synthetic minimal yeast promoters. Nat Commun. 2015;6:7810.
31. Tang H, Wu Y, Deng J, Chen N, Zheng Z, Wei Y, Luo X, Keasling JD. Promoter Architecture and promoter Engineering in Saccharomyces cerevisiae. Metabolites 2020, 10.
32. Liu L, Liu J, Qiu RX, Zhu XG, Dong ZY, Tang GM. Improving heterologous gene expression in Aspergillus Niger by introducing multiple copies of protein-binding sequence containing CCAAT to the promoter. Lett Appl Microbiol. 2003;36:358–61.
33. Zhang H, Yan JN, Zhang H, Liu TQ, Xu Y, Zhang YY, Li J. Effect of gpd box copy numbers in the gpdA promoter of aspergillus nidulans on its transcription efficiency in Aspergillus Niger. FEMS Microbiol Lett 2018, 365.
34. Minetoki T, Kumagai C, Gomi K, Kitamoto K, Takahashi K. Improvement of promoter activity by the introduction of multiple copies of the conserved region III sequence, involved in the efficient expression of aspergillus oryzae amylase-encoding genes. Appl Microbiol Biotechnol. 1998;50:459–67.
35. Zhang LH, Zheng XM, Cairns TC, Zhang ZD, Wang DP, Zheng P, Sun JB. Disruption or reduced expression of the orotidine-5 '-decarboxylase gene pyrG increases citric acid production: a new discovery during recyclable genome editing in Aspergillus niger. Microb Cell Fact 2020, 19.
36. Carvalho ND, Arentshorst M, Jin Kwon M, Meyer V, Ram AF. Expanding the ku70 toolbox for filamentous fungi: establishment of complementation vectors and recipient strains for advanced gene analyses. Appl Microbiol Biotechnol. 2010;87:1463–73.
37. Zheng X, Cairns T, Zheng P, Meyer V, Sun J. Protocol for gene characterization in Aspergillus Niger using 5S rRNA-CRISPR-Cas9-mediated Tet-on inducible promoter exchange. STAR Protoc. 2022;3:101838.
38. Zheng X, Yu J, Cairns TC, Zhang L, Zhang Z, Zhang Q, Zheng P, Sun J, Ma Y. Comprehensive Improvement of Sample Preparation methodologies facilitates dynamic metabolomics of Aspergillus Niger. Biotechnol J. 2019;14:e1800315.
39. Zheng X, Du P, Gao K, Du Y, Cairns TC, Ni X, Chen M, Zhao W, Ma X, Yang H, et al. Genome-wide transcription landscape of citric acid producing aspergillus Niger in response to glucose gradient. Front Bioeng Biotechnol. 2023;11:1282314.
40. Steiger MG, Rassinger A, Mattanovich D, Sauer M. Engineering of the citrate exporter protein enables high citric acid production in Aspergillus Niger. Metab Eng. 2019;52:224–31.
41. Xiao C, Liu X, Pan Y, Li Y, Qin L, Yan Z, Feng Y, Zhao M, Huang M. Tailored UPRE2 variants for dynamic gene regulation in yeast. Proc Natl Acad Sci U S A. 2024;121:e2315729121.
42. Wang Y, Liu R, Liu H, Li X, Shen L, Zhang W, Song X, Liu W, Liu X, Zhong Y. Development of a powerful synthetic hybrid promoter to improve the

cellulase system of Trichoderma reesei for efficient saccharification of corncob residues. Microb Cell Fact. 2022;21:5.
43. Cox JR, Fox A, Lenahan C, Pivnik L, Manion M, Blazeck J. Engineering CREB-activated promoters for adenosine-induced gene expression. Biotechnol J. 2024;19:e2300446.
44. Rantasalo A, Landowski CP, Kuivanen J, Korppoo A, Reuter L, Koivistoinen O, Valkonen M, Penttila M, Jantti J, Mojzita D. A universal gene expression system for fungi. Nucleic Acids Res. 2018;46:e111.

Publisher's note